Milcom 05 paper ID=1226

DATA FORMAT CLASSIFICATION FOR AUTONOMOUS SOFTWARE DEFINED RADIOS

Marvin Simon, Dariush Divsalar
Jet Propulsion Laboratory, California Institute of Technology
4800 Oak Grove Drive
Pasadena, California 91109
Marvin.K.Simon@jpl.nasa.gov, Dariush.Divsalar@jpl.nasa.gov

ABSTRACT

We present maximum-likelihood (ML) coherent and noncoherent classifiers for discriminating between NRZ and Manchester coded (biphase-L) data formats for binary phase-shift-keying (BPSK) modulation. Such classification of the data format is an essential element of so-called *autonomous* software defined radio (SDR) receivers (similar to so-called *cognitive* SDR receivers in the military application) where it is desired that the receiver perform each of its functions by extracting the appropriate knowledge from the received signal and, if possible, with as little information of the other signal parameters as possible. Small and large SNR approximations to the ML classifiers are also proposed that lead to simpler implementation with comparable performance in their respective SNR regions. Numerical performance results obtained by a combination of computer simulation and, wherever possible, theoretical analyses, are presented and comparisons are made among the various configurations based on the probability of misclassification as a performance criterion. Extensions to other modulations such as QPSK are readily accomplished using the same methods described in the paper.

INTRODUCTION

In autonomous radio operation, aside from classifying the modulation type, e.g, deciding between BPSK and QPSK, it is also desirable to have an algorithm for choosing the data format, e.g., NRZ versus Manchester encoding. In the absence of subcarriers, when NRZ is employed the carrier must be fully suppressed whereas Manchester coding allows for the possibility of a residual carrier, if desired. With this consideration in mind, there exist two different scenarios. In one case, independent of the data format, the modulations are assumed to be fully suppressed carrier. In the other case, which due to space limitations will be not be considered here, an NRZ data format is always used on a fully suppressed carrier modulation whereas a residual carrier modulation always employs Manchester coded data. In this case, the data format classification algorithm and its performance will clearly be a function of the modulation index, i.e., the allocation of the power to the discrete and data-modulated signal components. In this paper, we derive the maximum-likelihood (ML)-based data format classification algorithms as well as reduced complexity versions of them obtained by applying suitable approximations of the nonlinearities resulting from the ML formulation. As in previous classification problems of this type, we shall first assume that all other system parameters are known. Following this, we relax the assumption of known carrier phase and, as was done for the modulation classification investigation, we shall consider the noncoherent version of the ML classifiers. Numerical performance evaluation will be obtained by computer simulations and, wherever possible, by theoretical analyses to verify the simulation results.

MAXIMUM-LIKELIHOOD COHERENT CLASSIFIER OF DATA FORMAT FOR BPSK

We begin by considering suppressed carrier BPSK modulation and a choice between NRZ and Manchester encoding. Thus, the received signal is given by

$$r(t)=\sqrt{2P}\left(\sum_{n=-\infty}^{\infty}a_n p\left(t-nT_b\right)\right)\cos\omega_c t+n(t) \quad (1)$$

where P is the signal power, $\{a_n\}$ is the sequence of binary independent, identically distributed (i.i.d.) data taking on values ± 1 with equal probability, $p(t)$ is the pulse shape (the item to be classified), ω_c is the radian carrier frequency and $n(t)$ is a bandpass additive white Gaussian noise (AWGN) source with single-sided power spectral density N_0 W/Hz. Based on the above AWGN model, then for an observation of K_b bit intervals, the conditional likelihood function (CLF) is given by

$$p\left(r(t)\middle|\{a_n\},p(t)\right)$$

$$=\frac{1}{\sqrt{\pi N_0}}\exp\left(-\frac{1}{N_0}\int_0^{K_bT_b}\left[r(t)-\sqrt{2P}\left(\sum_{n=-\infty}^{\infty}a_n p\left(t-nT_b\right)\right)\cos\omega_c t\right]^2 dt\right) \quad (2)$$

$$=C\prod_{k=0}^{K_b-1}\exp\left(\frac{2\sqrt{2P}}{N_0}a_k\int_{kT_b}^{(k+1)T_b}r(t)p\left(t-kT_b\right)\cos\omega_c t dt\right)$$

where C is a constant that has no bearing on the classification. Averaging over the i.i.d. data sequence gives

$$p\left(r(t)\middle|p(t)\right)=C\prod_{k=0}^{K_b-1}\cosh\left(\frac{2\sqrt{2P}}{N_0}\int_{kT_b}^{(k+1)T_b}r(t)p\left(t-kT_b\right)\cos\omega_c t dt\right) \quad (3)$$

Finally, taking the logarithm of (3), we obtain the log-likelihood function (LLF)

$$\Lambda\triangleq\ln p\left(r(t)\middle|p(t)\right)=\sum_{k=0}^{K_b-1}\ln\cosh\left(\frac{2\sqrt{2P}}{N_0}\int_{kT_b}^{(k+1)T_b}r(t)p(t-kT)\cos\omega_c t dt\right) \quad (4)$$

where we have ignored the additive constant $\ln C$.

For NRZ data, $p(t)$ is a unit rectangular pulse of duration T_b, i.e,

$$p_1(t)=\begin{cases}1, 0\le t\le T_b\\ 0, \text{otherwise}\end{cases} \quad (5)$$

For Manchester encoded data, $p(t)$ is a unit square-wave pulse of duration T_b, i.e,

$$p_2(t)=\begin{cases}1, 0\le t\le T_b/2\\ -1, T_b/2\le t\le T_b\end{cases} \quad (6)$$

Thus, defining the received observables

$$r_k(l)\triangleq\int_{kT_b}^{(k+1)T_b}r(t)p_l\left(t-kT_b\right)\cos\omega_c t dt$$

$$=\begin{cases}\int_{kT_b}^{(k+1)T_b}r(t)\cos\omega_c t dt; l=1\\ \int_{kT_b}^{(k+1/2)T_b}r(t)\cos\omega_c t dt-\int_{(k+1/2)T_b}^{(k+1)T_b}r(t)\cos\omega_c t dt; l=2\end{cases} \quad (7)$$

then a classification choice between the two pulses shapes based on the LLF would be to choose Manchester if

$$\sum_{k=0}^{K_b-1}\ln\cosh\left(\frac{2\sqrt{2P}}{N_0}r_k(1)\right)<\sum_{k=0}^{K_b-1}\ln\cosh\left(\frac{2\sqrt{2P}}{N_0}r_k(2)\right) \quad (8)$$

Otherwise, choose NRZ.

REDUCED COMPLEXITY DATA FORMAT BPSK CLASSIFIERS

To simplify the form of the classification rule in (8), we replace the $\ln\cosh(\cdot)$ function by its small and large argument approximations. In particular,

$$\ln\cosh x\cong\begin{cases}x^2/2; x \text{ small}\\ |x|-\ln 2; x \text{ large}\end{cases} \quad (9)$$

Thus, for low SNR, (8) simplifies to

$$\sum_{k=0}^{K_b-1}\left(\int_{kT_b}^{(k+1)T_b}r(t)\cos\omega_c t dt\right)^2$$

$$<\sum_{k=0}^{K_b-1}\left(\int_{kT_b}^{(k+1/2)T_b}r(t)\cos\omega_c t dt-\int_{(k+1/2)T_b}^{(k+1)T_b}r(t)\cos\omega_c t dt\right)^2 \quad (10)$$

or, equivalently

$$\sum_{k=0}^{K_b-1}\int_{kT_b}^{(k+1/2)T_b}r(t)\cos\omega_c t dt\int_{(k+1/2)T_b}^{(k+1)T_b}r(\tau)\cos\omega_c\tau d\tau<0 \quad (11)$$

For high SNR, (8) reduces to

$$\sum_{k=0}^{K_b-1}\left|\int_{kT_b}^{(k+1/2)T_b}r(t)\cos\omega_c t dt+\int_{(k+1/2)T_b}^{(k+1)T_b}r(t)\cos\omega_c t dt\right|$$

$$<\sum_{k=0}^{K_b-1}\left|\int_{kT_b}^{(k+1/2)T_b}r(t)\cos\omega_c t dt-\int_{(k+1/2)T_b}^{(k+1)T_b}r(t)\cos\omega_c t dt\right| \quad (12)$$

Note that while the optimum classifier of (8) requires knowledge of SNR, the reduced-complexity classifiers of (10) and (12) do not. Figure 1 is a block diagram of the implementation of the low and high SNR classifiers defined by (11) and (12).

PROBABILITY OF MISCLASSIFICATION FOR COHERENT BPSK

To illustrate the behavior of the misclassification probability, P_M, with signal-to-noise ratio (SNR), we consider the low SNR case and evaluate first the probability of the event in (11) given that the transmitted data sequence was in fact NRZ encoded. In particular, we recognize that given a particular data sequence of K_b bits, $X_{ck}=\int_{kT_b}^{(k+1/2)T_b}r(t)\cos\omega_c t dt$, $Y_{ck}=\int_{(k+1/2)T_b}^{(k+1)T_b}r(\tau)\cos\omega_c\tau d\tau$; $k=0,1,\ldots,K_b-1$ are mutually independent and identically distributed (i.i.d.) Gaussian random variables (RVs). Thus, the LLF

$$D=\sum_{k=0}^{K_b-1}\int_{kT_b}^{(k+1/2)T_b}r(t)\cos\omega_c t dt\int_{(k+1/2)T_b}^{(k+1)T_b}r(\tau)\cos\omega_c\tau d\tau$$

$$=\sum_{k=0}^{K_b-1}X_{ck}Y_{ck} \quad (13)$$

is a special case of a quadratic form of *real* Gaussian RVs and the probability of the event in (11), namely, $\Pr\{D<0\}$ can be evaluated in closed form by applying the results in [1, Appendix B] and the additional simplification of these in [2, Appendix 9A]. To see this connection, we define the complex Gaussian RVs $X_k=X_{ck}+jX_{c,k+1}$, $Y_k=Y_{ck}+jY_{c,k+1}$. Then, the complex quadratic form $X_kY_k^*+X_k^*Y_k$. is equal to $2\left(X_{ck}Y_{ck}+X_{c,k+1}Y_{c,k+1}\right)$. Arbitrarily assuming K_b is even, then we can rewrite D of (13) as

$$D=\frac{1}{2}\sum_{k=0}^{K_b/2-1}\left(X_kY_k^*+X_k^*Y_k\right) \tag{14}$$

Comparing (14) with [1, Eq. (B.1)] we see that the former is a special case of the latter corresponding to $A=B=0, C=1/2$. Specifically, making use of the first and second moments of X_k and Y_k given by

$$\begin{aligned}\overline{X}_k&=\overline{Y}_k=(a_k+ja_{k+1})\sqrt{P/8}T_b\\ \mu_{xx}&=\frac{1}{2}E\left\{\left|X_k-\overline{X}_k\right|^2\right\}=N_0T_b/8\\ \mu_{yy}&=\frac{1}{2}E\left\{\left|Y_{ck}-\overline{Y}_{ck}\right|^2\right\}=N_0T_b/8\\ \mu_{xy}&=\frac{1}{2}E\left\{\left(X_{ck}-\overline{X}_{ck}\right)\left(Y_{ck}-\overline{Y}_{ck}\right)^*\right\}=0\end{aligned} \tag{15}$$

then from [2, Eq. (9A.15)]

$$P_M(1)=\frac{1}{2}+\frac{1}{2^{K_b-1}}\sum_{k=1}^{K_b/2}\binom{K_b-1}{K_b/2-k}\left[Q_k(a,b)-Q_k(b,a)\right] \tag{16}$$

where $Q_k(a,b)$ is the kth-order Marcum Q-function and

$$a=\sqrt{\frac{\nu\left(\xi_1\nu-\xi_2\right)}{2}},\ b=\sqrt{\frac{\nu\left(\xi_1\nu+\xi_2\right)}{2}} \tag{17}$$

with

$$\begin{aligned}\nu&=\sqrt{\frac{1}{\mu_{xx}\mu_{yy}}}=\frac{8}{N_0T_b}\\ \xi_1&=\frac{1}{2}\sum_{k=0}^{K_b/2-1}\left(\left|\overline{X}_{ck}\right|^2\mu_{yy}+\left|\overline{Y}_{ck}\right|^2\mu_{xx}\right)=K_b\frac{PT_b^3N_0}{64}\\ \xi_2&=\sum_{k=0}^{K_b/2-1}\left|\overline{X}_{ck}\right|\left|\overline{Y}_{ck}\right|=K_b\frac{PT_b^2}{8}\end{aligned} \tag{18}$$

Substituting (18) into (17) gives

$$a=0,\ b=\sqrt{K_b\left(PT_b/N_0\right)}=\sqrt{K_b\left(E_b/N_0\right)} \tag{19}$$

However,

$$\begin{aligned}Q_k(0,b)&=\sum_{n=0}^{k-1}\exp\left(-\frac{b^2}{2}\right)\frac{\left(b^2/2\right)^n}{n!}\\ Q_k(b,0)&=1\end{aligned} \tag{20}$$

Thus, using (19) and (20) in (16) gives the desired result

$$P_M(1)=\frac{1}{2}+\frac{1}{2^{K_b-1}}\sum_{k=1}^{K_b/2}\binom{K_b-1}{K_b/2-k}\times\left[\sum_{n=0}^{k-1}\exp\left(-\frac{K_bE_b}{2N_0}\right)\frac{\left(K_bE_b/2N_0\right)^n}{n!}-1\right] \tag{21}$$

Noting that

$$\sum_{k=1}^{K_b/2}\binom{K_b-1}{K_b/2-k}=2^{K_b-2} \tag{22}$$

then (21) further simplifies to

$$P_M(1)=\frac{1}{2^{K_b-1}}\sum_{k=1}^{K_b/2}\binom{K_b-1}{K_b/2-k}\sum_{n=0}^{k-1}\exp\left(-\frac{K_bE_b}{2N_0}\right)\frac{\left(K_bE_b/2N_0\right)^n}{n!} \tag{23}$$

To compute the probability of choosing NRZ when in fact Manchester is the true encoding, we need to evaluate $\Pr\{D\ge 0\}=1-\Pr\{D<0\}$ when instead of (15) we have

$$\begin{aligned}\overline{X}_k&=(a_k+ja_{k+1})\sqrt{P/8}T_b\\ \overline{Y}_k&=-(a_k+ja_{k+1})\sqrt{P/8}T_b\end{aligned} \tag{24}$$

Since the impact of the negative mean for $\overline{Y}_k$ in (24) is to reverse the sign of ξ_2 in (18), then we immediately conclude that for this case the values of a and b in (19) merely switch roles, i.e.,

$$a=\sqrt{K_b\left(E_b/N_0\right)},\ b=0 \tag{25}$$

Substituting these values in (16) now gives

$$P_M(2)=1-\left\{\frac{1}{2}+\frac{1}{2^{K_b-1}}\sum_{k=1}^{K_b/2}\binom{K_b-1}{K_b/2-k}\times\left[1-\sum_{n=0}^{k-1}\exp\left(-\frac{K_bE_b}{2N_0}\right)\frac{\left(K_bE_b/2N_0\right)^n}{n!}\right]\right\} \tag{26}$$

which again simplifies to

$$P_M(2)=\frac{1}{2^{K_b-1}}\sum_{k=1}^{K_b/2}\binom{K_b-1}{K_b/2-k}\sum_{n=0}^{k-1}\exp\left(-\frac{K_bE_b}{2N_0}\right)\frac{\left(K_bE_b/2N_0\right)^n}{n!} \tag{27}$$

Since (23) and (27) are identical, the average probability of mismatch, P_M is then either of the two results.

Illustrated in Fig. 2 are numerical results for the misclassification probability obtained by computer simulation for the optimum and reduced-complexity data format classifiers as given by (8), (11) and (12). Also illustrated are the numerical results obtained from the closed-form analytical solution given in (23) for the low SNR reduced-complexity scheme. As can be seen, the agreement between theoretical and simulated results is exact. Furthermore, the difference in performance between the optimum and reduced-complexity classifiers is quite small over a large range of SNRs.

MAXIMUM-LIKELIHOOD NONCOHERENT CLASSIFIER OF DATA FORMAT FOR BPSK

Here we assume that the carrier has a random phase, θ, that is unknown and uniformly distributed. Thus, the received signal of (1) is now modeled as

$$r(t)=\sqrt{2P}\left(\sum_{n=-\infty}^{\infty}a_np(t-nT_b)\right)\cos(\omega_ct+\theta)+n(t) \tag{28}$$

and the corresponding CLF becomes

$$\begin{aligned}&p\left(r(t)\middle|\{a_n\},p(t),\theta\right)\\ &=C\prod_{k=0}^{K_b-1}\exp\left(\frac{2\sqrt{2P}}{N_0}a_k\int_{kT_b}^{(k+1)T_b}r(t)p(t-kT_b)\cos(\omega_ct+\theta)dt\right)\end{aligned} \tag{29}$$

At this point we have the option of first averaging over the random carrier phase and then the data or vice versa. Considering the first option, we start by rewriting (29) as

$$p\left(r(t)\middle|\{a_n\},p(t),\theta\right) = C\exp\left(\frac{2\sqrt{2P}}{N_0}\sqrt{\left(\sum_{k=0}^{K_b-1}a_k r_{ck}\right)^2+\left(\sum_{k=0}^{K_b-1}a_k r_{sk}\right)^2}\cos(\theta+\eta)\right); \quad (30)$$

$$\eta = \tan^{-1}\frac{\sum_{k=0}^{K_b-1}a_k r_{sk}}{\sum_{k=0}^{K_b-1}a_k r_{ck}}$$

Averaging over the carrier phase results in (ignoring constants)

$$p\left(r(t)\middle|\{a_n\},p(t)\right) = I_0\left(\frac{2\sqrt{2P}}{N_0}\sqrt{\left(\sum_{k=0}^{K_b-1}a_k r_{ck}\right)^2+\left(\sum_{k=0}^{K_b-1}a_k r_{sk}\right)^2}\right) \quad (31)$$

where $I_0(\cdot)$ is the zero order modified Bessel function of the first kind. Unfortunately, the average over the data sequence cannot be obtained in closed form. Hence, the classification algorithm can only be stated as follows: Given that NRZ was transmitted, choose the Manchester format if

$$E_{\mathbf{a}}\left\{I_0\left(\frac{2\sqrt{2P}}{N_0}\sqrt{\left(\sum_{k=0}^{K_b-1}a_k r_{ck}(1)\right)^2+\left(\sum_{k=0}^{K_b-1}a_k r_{sk}(1)\right)^2}\right)\right\} < E_{\mathbf{a}}\left\{I_0\left(\frac{2\sqrt{2P}}{N_0}\sqrt{\left(\sum_{k=0}^{K_b-1}a_k r_{ck}(2)\right)^2+\left(\sum_{k=0}^{K_b-1}a_k r_{sk}(2)\right)^2}\right)\right\} \quad (32)$$

where $E_{\mathbf{a}}\{\cdot\}$ denotes expectation over the data sequence $\mathbf{a}=(a_0,a_1,...,a_{K_b-1})$. Otherwise, choose NRZ.

Consider now the second option where we first average over the data sequence. Then,

$$p\left(r(t)|p(t),\theta\right) = C\prod_{k=0}^{K_b-1}E_{a_k}\left\{\exp\left(\frac{2\sqrt{2P}}{N_0}a_k\int_{kT_b}^{(k+1)T_b}r(t)p(t-kT_b)\cos(\omega_c t+\theta)dt\right)\right\}$$

$$= C\exp\left[\sum_{k=0}^{K_b-1}\ln\cosh\left(\frac{2\sqrt{2P}}{N_0}\int_{kT_b}^{(k+1)T_b}r(t)p(t-kT_b)\cos(\omega_c t+\theta)dt\right)\right] \quad (33)$$

Thus, a classification between NRZ and Manchester encoding would be based on a comparison of

$$E_\theta\left\{\exp\left[\sum_{k=0}^{K_b-1}\ln\cosh\left(\frac{2\sqrt{2P}}{N_0}\int_{kT_b}^{(k+1)T_b}r(t)p_1(t-kT_b)\cos(\omega_c t+\theta)dt\right)\right]\right\}$$

with

$$E_\theta\left\{\exp\left[\sum_{k=0}^{K_b-1}\ln\cosh\left(\frac{2\sqrt{2P}}{N_0}\int_{kT_b}^{(k+1)T_b}r(t)p_2(t-kT_b)\cos(\omega_c t+\theta)dt\right)\right]\right\}$$

To simplify matters, before averaging over the carrier phase, one must employ the approximations to the nonlinearities given in (9). In particular, for low SNR we have

$$p\left(r(t)|p(t)\right) = E_\theta\left\{\exp\left[\frac{1}{2}\sum_{k=0}^{K_b-1}\left(\frac{2\sqrt{2P}}{N_0}\int_{kT_b}^{(k+1)T_b}r(t)p(t-kT_b)\cos(\omega_c t+\theta)dt\right)^2\right]\right\}$$

$$= \exp\left[\frac{2P}{N_0^2}\sum_{k=0}^{K_b-1}\left(r_{ck}^2+r_{sk}^2\right)\right] \times I_0\left(\frac{2P}{N_0^2}\sqrt{\left(\sum_{k=0}^{K_b-1}\left(r_{ck}^2+r_{sk}^2\right)\cos 2\eta_k\right)^2+\left(\sum_{k=0}^{K_b-1}\left(r_{ck}^2+r_{sk}^2\right)\sin 2\eta_k\right)^2}\right) \quad (34)$$

where

$$\eta_k = \tan^{-1}\frac{r_{sk}}{r_{ck}} \quad (35)$$

Thus, since

$$\cos 2\eta_k = \frac{r_{ck}^2-r_{sk}^2}{r_{ck}^2+r_{sk}^2}, \quad \sin 2\eta_k = \frac{2r_{ck}r_{sk}}{r_{ck}^2+r_{sk}^2} \quad (36)$$

we finally have

$$p\left(r(t)|p(t)\right) = \exp\left[\frac{2P}{N_0^2}\sum_{k=0}^{K_b-1}\left(r_{ck}^2+r_{sk}^2\right)\right]I_0\left(\frac{2P}{N_0^2}\left|\sum_{k=0}^{K_b-1}\tilde{r}_k^2\right|\right) \quad (37)$$

where

$$\tilde{r}_k \triangleq r_{ck}+jr_{sk} = \int_{kT_b}^{(k+1)T_b}r(t)p(t-kT_b)e^{j\omega_c t}dt \quad (38)$$

Finally then, the classification decision rule analogous to (32) is: Given that NRZ data was transmitted, decide on Manchester coding if

$$\exp\left[\frac{2P}{N_0^2}\sum_{k=0}^{K_b-1}\left|\tilde{r}_k(1)\right|^2\right]I_0\left(\frac{2P}{N_0^2}\left|\sum_{k=0}^{K_b-1}\tilde{r}_k^2(1)\right|\right) < \exp\left[\frac{2P}{N_0^2}\sum_{k=0}^{K_b-1}\left|\tilde{r}_k(2)\right|^2\right]I_0\left(\frac{2P}{N_0^2}\left|\sum_{k=0}^{K_b-1}\tilde{r}_k^2(2)\right|\right) \quad (39)$$

Equivalently, normalizing the observables to

$$\tilde{r}_k' \triangleq \frac{1}{T_b}\int_{kT_b}^{(k+1)T_b}\frac{r(t)}{\sqrt{2P}}p(t-kT_b)e^{j\omega_c t}dt \quad (40)$$

then (39) becomes

$$\exp\left[\left(\frac{2E_b}{N_0}\right)^2\sum_{k=0}^{K_b-1}\left|\tilde{r}_k'(1)\right|^2\right]I_0\left(\left(\frac{2E_b}{N_0}\right)^2\left|\sum_{k=0}^{K_b-1}\tilde{r}_k'^2(1)\right|\right) < \exp\left[\left(\frac{2E_b}{N_0}\right)^2\sum_{k=0}^{K_b-1}\left|\tilde{r}_k'(2)\right|^2\right]I_0\left(\left(\frac{2E_b}{N_0}\right)^2\left|\sum_{k=0}^{K_b-1}\tilde{r}_k'^2(2)\right|\right) \quad (41)$$

Since we have already assumed low SNR in arriving at (41), we can further approximate the

nonlinearities in that equation by their values for small arguments. Retaining only linear terms, we arrive at the simplification

$$\sum_{k=0}^{K_b-1}\left|\tilde{r}_k'(1)\right|^2 < \sum_{k=0}^{K_b-1}\left|\tilde{r}_k'(2)\right|^2 \tag{42}$$

or, equivalently

$$\sum_{k=0}^{K_b-1}\left|\tilde{r}_k(1)\right|^2 < \sum_{k=0}^{K_b-1}\left|\tilde{r}_k(2)\right|^2 \tag{43}$$

which again does not require knowledge of SNR. On the other hand, if we retain second-order terms, then (41) simplifies to

$$\begin{aligned}&\sum_{k=0}^{K_b-1}\left|\tilde{r}_k'(1)\right|^2+\frac{1}{4}\left(\frac{2E_b}{N_0}\right)^2\left[2\left(\sum_{k=0}^{K_b-1}\left|\tilde{r}_k'(1)\right|^2\right)^2+\left|\sum_{k=0}^{K_b-1}\tilde{r}_k'^2(1)\right|^2\right]\\ &<\sum_{k=0}^{K_b-1}\left|\tilde{r}_k'(2)\right|^2+\frac{1}{4}\left(\frac{2E_b}{N_0}\right)^2\left[2\left(\sum_{k=0}^{K_b-1}\left|\tilde{r}_k'(2)\right|^2\right)^2+\left|\sum_{k=0}^{K_b-1}\tilde{r}_k'^2(2)\right|^2\right]\end{aligned} \tag{44}$$

which is SNR-dependent.

Expanding (43) in the form of (10), we obtain

$$\begin{aligned}&\sum_{k=0}^{K_b-1}\left(\int_{kT_b}^{(k+1)T_b}r(t)\cos\omega_c t dt\right)^2+\left(\int_{kT_b}^{(k+1)T_b}r(t)\sin\omega_c t dt\right)^2\\ &<\sum_{k=0}^{K_b-1}\left(\int_{kT_b}^{(k+1/2)T_b}r(t)\cos\omega_c t dt-\int_{(k+1/2)T_b}^{(k+1)T_b}r(t)\cos\omega_c t dt\right)^2\\ &+\sum_{k=0}^{K_b-1}\left(\int_{kT_b}^{(k+1/2)T_b}r(t)\sin\omega_c t dt-\int_{(k+1/2)T_b}^{(k+1)T_b}r(t)\sin\omega_c t dt\right)^2\end{aligned} \tag{45}$$

or

$$\mathrm{Re}\left\{\sum_{k=0}^{K_b-1}\int_{kT_b}^{(k+1/2)T_b}r(t)e^{j\omega_c t}dt\int_{(k+1/2)T_b}^{(k+1)T_b}r(\tau)e^{-j\omega_c t}d\tau\right\}<0 \tag{46}$$

which is the analogous result to (11) for the coherent case.

For high SNR, even after applying the approximations to the nonlinearities given in (9), it is still difficult to average over the random carrier phase. Instead, we take note of the resemblance between (46) and (11) for the low SNR case and propose an ad hoc complex equivalent to (12) for the noncoherent high SNR case, namely,

$$\begin{aligned}&\sum_{k=0}^{K_b-1}\left|\int_{kT_b}^{(k+1/2)T_b}r(t)e^{j\omega_c t}dt+\int_{(k+1/2)T_b}^{(k+1)T_b}r(t)e^{j\omega_c t}dt\right|\\ &<\sum_{k=0}^{K_b-1}\left|\int_{kT_b}^{(k+1/2)T_b}r(t)e^{j\omega_c t}dt-\int_{(k+1/2)T_b}^{(k+1)T_b}r(t)e^{j\omega_c t}dt\right|\end{aligned} \tag{47}$$

Figure 3 is a block diagram of the implementation of the low and high SNR classifiers defined by (46) and (47).

PROBABILITY OF MISCLASSIFICATION FOR NONCOHERENT BPSK

To compute the probability of misclassification, we note that (46) is still made up of a sum of products of mutually independent real Gaussian RVs and thus can still be written in the form of (14) with twice as many terms, i.e.,

$$D=\frac{1}{2}\sum_{k=0}^{K_b-1}\left(X_kY_k^*+X_k^*Y_k\right) \tag{48}$$

where now the complex Gaussian RVs are defined as $X_k=X_{ck}+jX_{sk}$, $Y_k=Y_{ck}+jY_{sk}$. The means of the terms are given by

$$\overline{X}_k=\overline{Y}_k=a_k(\cos\theta-j\sin\theta)\sqrt{P/8}T_b \tag{49}$$

whereas the variances and crosscorrelations are the same as in (15). Thus, since the magnitude of the means in (49) is reduced by a factor of $\sqrt{2}$ relative to that of the means in (15), we conclude that the probability of misclassification is obtained from (23) by replacing E_b/N_0 with $E_b/2N_0$ and K_b with $2K_b$ resulting in

$$P_M=\frac{1}{2^{2K_b-1}}\sum_{k=1}^{K_b}\binom{2K_b-1}{K_b-k}\sum_{n=0}^{k-1}\exp\left(-\frac{K_bE_b}{2N_0}\right)\frac{\left(K_bE_b/2N_0\right)^n}{n!} \tag{50}$$

Fig. 4 illustrates numerical results for the misclassification probability obtained by computer simulation for the low SNR and high SNR reduced-complexity data format classifiers as specified by (46) and (47), respectively, as well as the optimum classifier described by the comparison below Eq. (33). Also illustrated are the numerical results obtained from the closed-form analytical solution given in (50) for the low SNR reduced-complexity scheme (which are in exact agreement with the simulation results). As in the coherent case, the difference in performance between the low and high SNR reduced-complexity classifiers is again quite small over a large range of SNRs. Furthermore, we see here again that the performances of the approximate but simpler classification algorithms are in close proximity to that of the optimum one. Finally, comparison between the corresponding coherent and noncoherent classifiers is illustrated in Fig. 5 and reveals a penalty of approximately 1 dB or less depending on the SNR.

ACKNOWLEDGEMENT

This research was carried out at the Jet Propulsion Laboratory, California Institute of Technology, under contract with the National Aeronautics and Space Administration.

REFERENCES

1. J. Proakis, Digital Communications, New York: McGraw-Hill, 4th ed., 2001.

2. M. K. Simon and M.-S. Alouini, *Digital Communication over Fading Channels: A Unified Approach to Performance Analysis*, 2nd ed., New York: John Wiley & Sons., 2005.

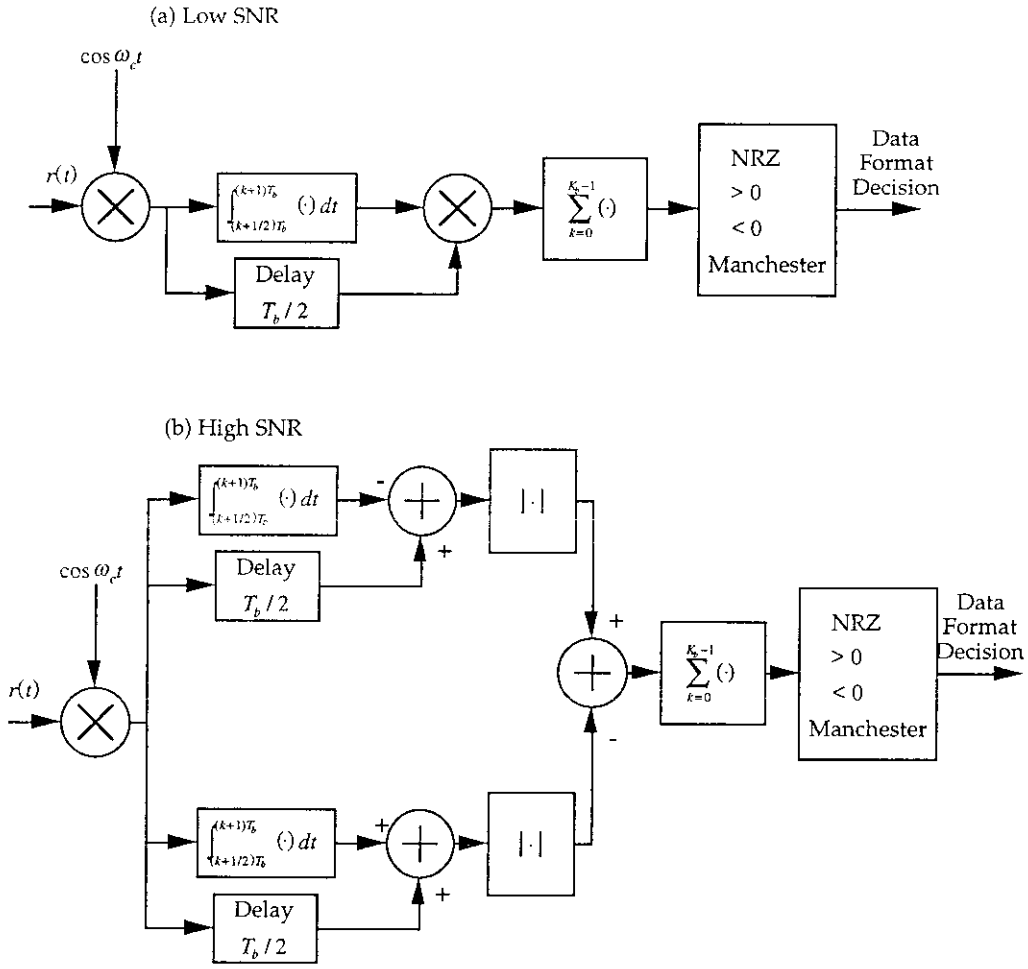

Fig. 1. Reduced Complexity Coherent Data Format Classifiers for BPSK Modulation

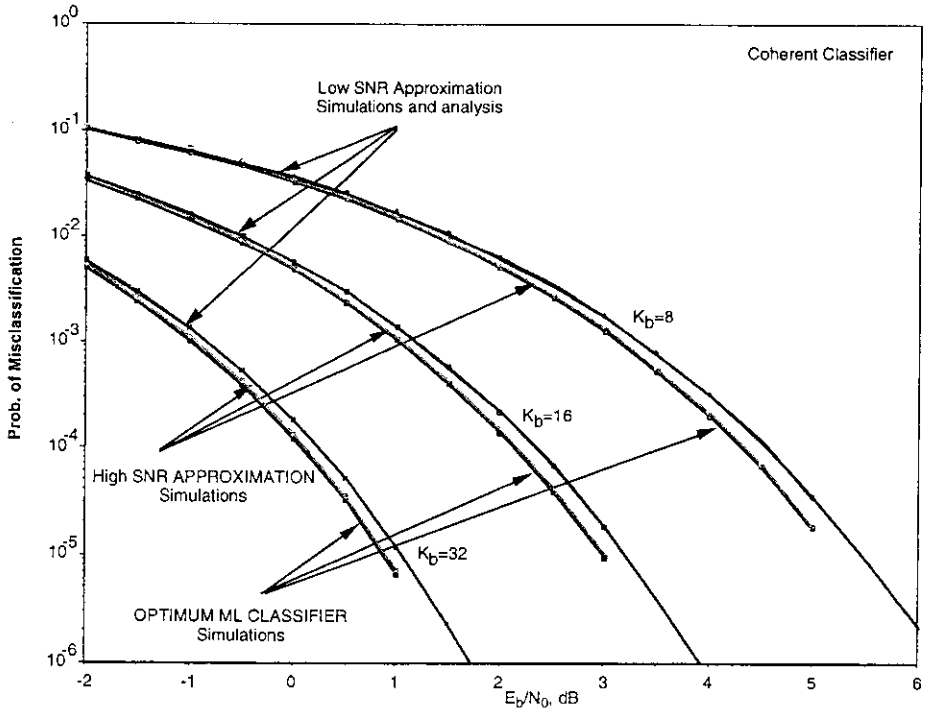

Fig. 2. A Comparison of the Performance of Coherent Data Format Classifiers for BPSK Modulation.

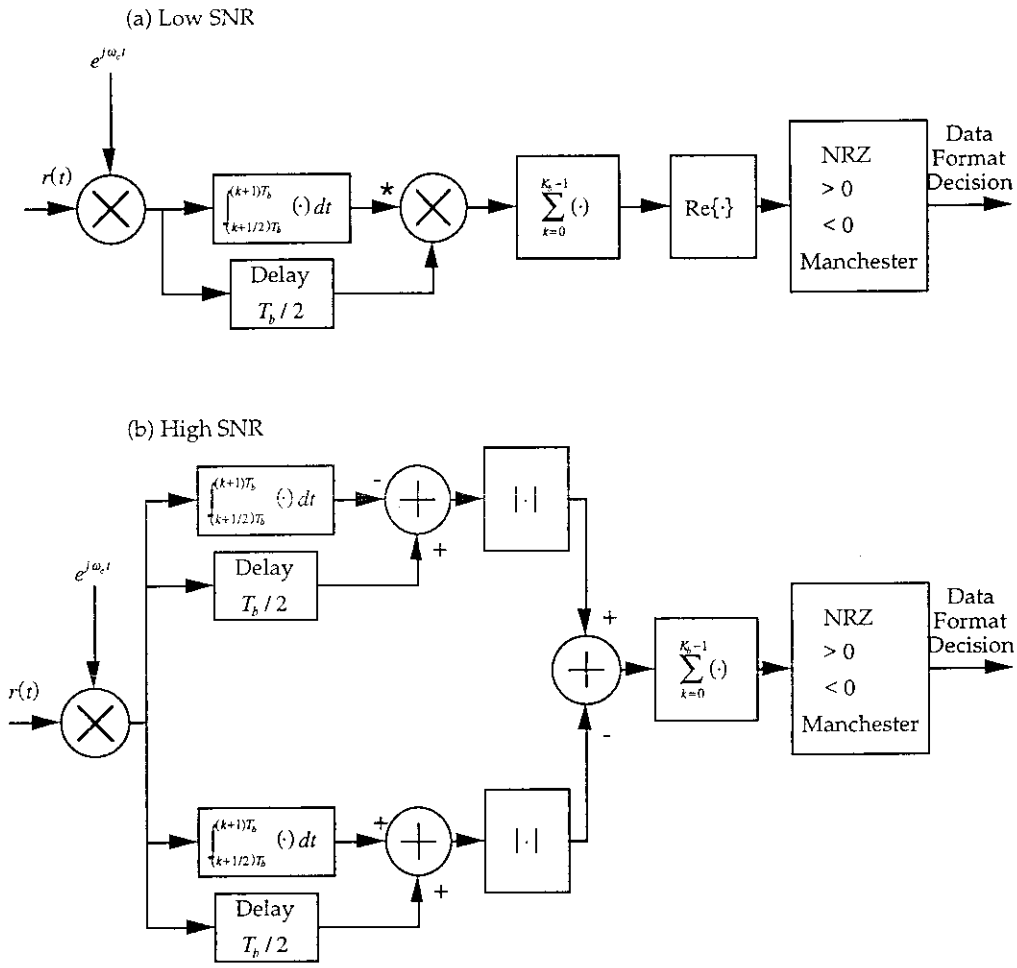

Fig. 3. Reduced Complexity Noncoherent Data Format Classifiers for BPSK Modulation

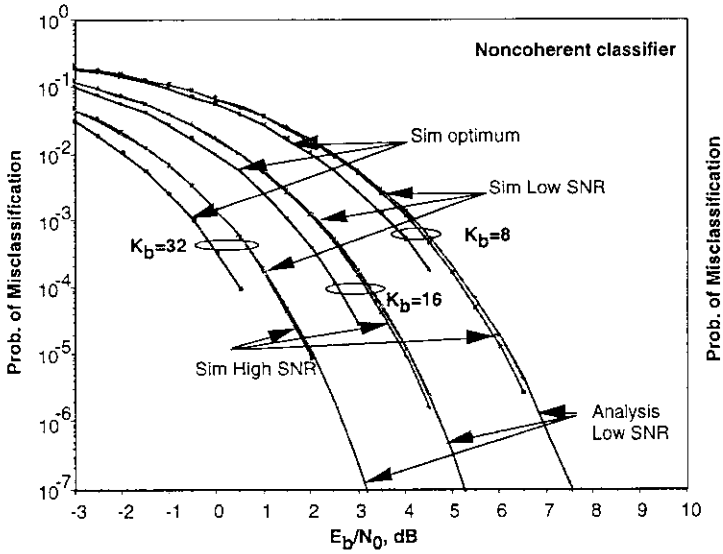

Fig. 4. A Comparison of the Performance of Noncoherent Data Format Classifiers for BPSK Modulation.

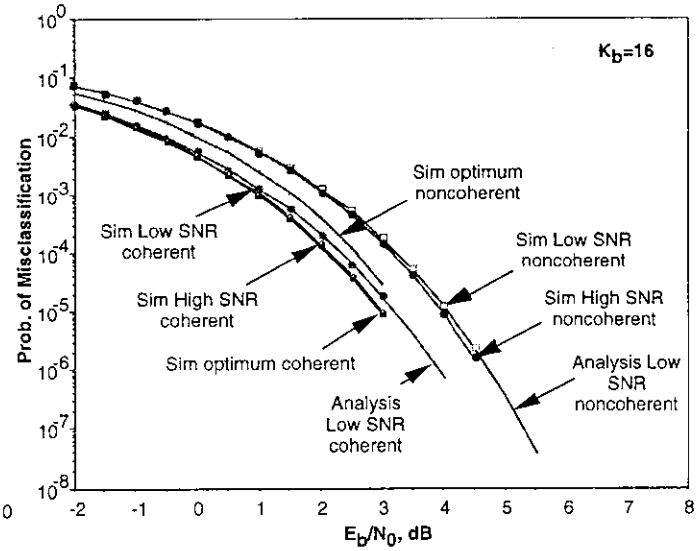

Fig. 5. A Comparison of the Performance of Coherent and Noncoherent Data Format Classifiers for BPSK Modulation.